

# Mnemosyne: Learning to Train Transformers with Transformers

Deepali Jain<sup>\* 1</sup> Krzysztof Marcin Choromanski<sup>\* 1 2</sup> Sumeet Singh<sup>1</sup> Vikas Sindhwani<sup>1</sup>  
 Tingnan Zhang<sup>1</sup> Jie Tan<sup>1</sup> Avinava Dubey<sup>1</sup>

## Abstract

Training complex machine learning (ML) architectures requires a compute and time consuming process of selecting the right optimizer and tuning its hyper-parameters. A new paradigm of learning optimizers from data has emerged as a better alternative to hand-designed ML optimizers. We propose *Mnemosyne*<sup>1</sup> optimizer, that uses Performers (Choromanski et al., 2021): implicit low-rank attention Transformers. It can learn to train entire neural network architectures including other Transformers without any task-specific optimizer tuning. We show that Mnemosyne: **(a)** generalizes better than popular LSTM optimizer, **(b)** in particular can successfully train Vision Transformers (ViTs) while meta-trained on standard MLPs and **(c)** can initialize optimizers for faster convergence in Robotics applications. We believe that these results open the possibility of using Transformers to build foundational optimization models that can address the challenges of regular Transformer training. We complement our results with an extensive theoretical analysis of the compact associative memory used by Mnemosyne.

## 1. Introduction

Learning-to-learn (L2L) systems (Thrun & Pratt, 1998; Sutton, 1992; Bengio et al., 1992; 1995; Naik & Mammone, 1992; Hochreiter et al., 2001; Santoro et al., 2016; Younger et al., 2001; Andrychowicz et al., 2016; Chen et al., 2021) used to train machine learning (ML) optimizers can be thought of as a natural lifting (to the optimizer-space) of the idea that has revolutionized ML: replacing hand-engineered features with learnable ones.

The idea to train ML optimizers is tempting, yet the lift to the optimizer-space comes at a price: the instances used to

<sup>\*</sup>Equal contribution <sup>1</sup>Google Robotics <sup>2</sup>Columbia University, NYC, NY, US. Correspondence to: Deepali Jain <jaindeepali@google.com>, Krzysztof Marcin Choromanski <kchoro@google.com>.

<sup>1</sup>Project page: <https://sites.google.com/view/mnemosyne-opt>

train such systems are the optimization problems themselves. Generalization in such a setting means: the ability to transfer knowledge to "similar" optimization tasks not seen in training. Rigorous mathematical analysis of the properties of L2L systems, that involves defining distributions over optimization problems, becomes challenging and is a subject on its own. Indeed, the literature on *meta-learning* is voluminous (Yao et al., 2022; Berseth et al., 2022; Pong et al., 2022; Zhao et al., 2020; Alet et al., 2018; Li et al., 2020; Fallah et al., 2021) and of critical importance in many disciplines such as Robotics, where transfer knowledge from simulator to hardware is a notoriously difficult problem (Liang et al., 2020; James et al., 2019; Ravi & Larochelle, 2017).

A standard approach to learning optimizers is to cast it as a *sequential decision problem*, where a function  $f$  called an *optimizee* is optimized via another function  $g_\theta$  (an optimizer) with learnable parameters  $\theta$ . Usually  $f$  takes as input  $\mathbf{x}$  the parameters of a particular neural network (NN) model under consideration and can output for instance its corresponding test loss on a given task. The optimizer  $g_\theta$  updates  $\mathbf{x}$  as:

$$\begin{cases} \mathbf{x}_0 \leftarrow \text{optimization initial point,} \\ \mathbf{x}_{t+1} = g_\theta(f, \mathbf{x}_0, \dots, \mathbf{x}_t) & \text{if } t > 0 \end{cases} \quad (1)$$

Function  $g_\theta$  is either trained by minimizing the meta-loss objective  $\mathcal{L}_\theta$  which is usually a sum of  $f$ -losses over certain time horizons with supervised/reinforcement learning (Li & Malik, 2017) or in a completely supervised way, where it learns to imitate expert-optimizers (Chen et al., 2020).

Function  $g_\theta$  usually does not act directly on the sequence  $(\mathbf{x}_0, \dots, \mathbf{x}_t)$ , but its processed-version, e.g. the sequence of the corresponding gradients  $(\nabla f(\mathbf{x}_0), \dots, \nabla f(\mathbf{x}_t))$  if  $f$  is differentiable (which does not need to be the case (Metz et al., 2019a)). In practice, the processed-versions have much richer structure (Metz et al., 2020): "...various rolling statistics including...loss data structures, the rolling momentum / rms terms, as well as the gradient clipping state...".

In this paper, we abstract from the low-level design of the sequential inputs to  $g_\theta$  (which is a subject on its own) and different training strategies of  $g_\theta$ . Our interest is in the core design of  $g_\theta$  since it acts as a memory-based system.

Indeed, most models of  $g_\theta$  leverage recurrent NN cells, such as LSTMs (Andrychowicz et al., 2016; Roy & Todorovic,

2018; Ravi & Larochelle, 2017), that keep the history of the optimization-rollout in the form of a compact learnable latent state. In addition, due to the fact that inputs  $\mathbf{x}$  to  $f$  are usually high-dimensional (e.g. neural networks' parameter-vectors),  $g_\theta$  is often factorized to process independently different dimensions of  $\mathbf{x}$  (Andrychowicz et al., 2016).

The Transformer-revolution in ML set the stage for a very different way to model sequential data and in general: to model memory - the *attention mechanism* (Vaswani et al., 2017; Chowdhery et al., 2022; Radford et al., 2019; Brown et al., 2020; Devlin et al., 2019; Chen et al., 2018). A natural question is whether Transformer-based architectures can be used to replace LSTM-based memory cells in L2L-systems.

Applying Transformers in this context is compelling - modeling long-range relationships over time by avoiding catastrophic forgetting (which is what LSTMs struggle with, but Transformers are particularly good at) is especially relevant for optimizing highly non-convex objectives in deep learning. However these benefits come at the cost of quadratic (in the sequence-length) space and time complexity.

**Contributions.** We propose a new paradigm, called *Mnemosyne*, for learning machine learning optimizers that applies Performers (Choromanski et al., 2021): implicit low-rank attention Transformers to encode memory-cells. It overcomes the quadratic complexity concerns of regular attention and can learn to train entire neural network architectures. We show that Mnemosyne: (a) generalizes better than popular LSTM optimizer, (b) in particular can successfully train Vision Transformers (ViTs) while meta-trained on standard MLPs and (c) can initialize optimizers for faster convergence in Robotics applications. We believe that these results open the possibility of using Transformers to build foundational optimization models that can address the challenges of optimizer tuning (see: Sec. 5.1).

Our considered model of using  $g_\theta$  is more general than the one presented in Eq. 1 and is of the form given below for  $g_\theta = (g_{\theta_1}^{\text{init}}, g_{\theta_2}^{\text{hist}})$ ,  $\theta = [\theta_1; \theta_2]$  and a *context-vector*  $\mathbf{c}$ :

$$\begin{cases} \mathbf{x}_0 = g_{\theta_1}^{\text{init}}(\mathbf{c}), \\ \mathbf{x}_{t+1} = g_{\theta_2}^{\text{hist}}(f, \mathbf{x}_0, \dots, \mathbf{x}_t) \quad \text{if } t > 0 \end{cases} \quad (2)$$

The optimizer  $g$  is now explicitly split into two-parts: (1)  $g_{\theta_1}^{\text{init}}$  that learns initial optimization point from the context-vector, e.g. the image encoding the scene (as it is the case in learnable-MPC setting (Xiao et al., 2022)), see: Sec. 5.2 and (2)  $g_{\theta_2}^{\text{hist}}$  that processes the history of the optimization steps, as we described before. Depending on the application, either one or the other optimizer (or both) are turned on. Critically, both are encoded as light scalable Transformers. Optimizer  $g_{\theta_1}^{\text{init}}$  applies spatial bi-directional attention while  $g_{\theta_2}^{\text{hist}}$  uses its causal (temporal) uni-directional variant.

Low-rank implicit Performer's attention guarantees **linear**

(in history-length and/or context-vector size) space and time complexity. It is used in the optimizer model as an effective *compact associative memory* (CAM) (see: Sec. 2). In the causal setting, it provides the best of both worlds: efficiency due to the compact fixed-size hidden state (as in LSTMs) and expressiveness since this hidden state approximates regular Transformer's attention via the CAS-mechanism.

We complement our results with an extensive theoretical analysis of the capacity of Mnemosyne's compact associative memory model (see: Sec. 4) that is interesting on its own and, to the best of our knowledge, has never been conducted before. All the proofs are given in the Appendix.

## 2. Related work

The research on L2L-systems involves a plethora of techniques: curriculum learning (e.g. incrementally increasing optimizer's unroll length (Chen et al., 2020)), randomly scaled optimizers in training with relative scaling of input gradients (Lv et al., 2017), hierarchical RNN-architectures with lower memory and compute overhead that are capable of capturing inter-parameter dependencies (Wichrowska et al., 2017) and more (Cao et al., 2019; Metz et al., 2019b; Chen et al., 2016; Vicol et al., 2021).

Regular transformers are being recently considered in this setting, in particular to tune hyperparameters (Chen et al., 2022), to learn BFGS-type optimization for motion reconstruction (Gärtner et al., 2022) or as memory-systems in class-incremental learning (Iszen et al., 2022).

Scalable Transformers (Tay et al., 2020; 2021) were born to address the computational limitations of regular Transformers. Several efficient attention mechanisms were proposed, based on hashing (Kitaev et al., 2020), graph clustering (Roy et al., 2021), dimensionality reduction (Wang et al., 2020) or sparse attention (Zaheer et al., 2020).

In this paper, we are primarily interested in methods approximating attention via low-rank decomposition of the attention matrix (Choromanski et al., 2021; Likhosherstov et al., 2022; Luo et al., 2021; Choromanski et al., 2022; Likhosherstov et al., 2020; Chowdhury et al., 2022), due to their intrinsic connection with associative memory and energy-models (Krotov & Hopfield, 2016). Regular Transformers can be thought of as differentiable dictionaries applying powerful *associative memory mechanisms* (Krotov & Hopfield, 2021; Ramsauer et al., 2020), i.e. modern Hopfield networks (Hopfield, 2007) with exponential memory. Linear low-rank attention mechanisms are their compact variants (Schlag et al., 2021) with intriguing theoretical properties and are perfect candidates for scalable memory-systems.

That interpretation has profound practical consequences. As we show in Sec. 5.1, Mnemosyne, which approximates modern Hopfield exponential memory (via the so-called

*hyperbolic cosine random features*), outperforms other algorithms when used to encode  $g_{\theta_2}^{\text{hist}}$ . Furthermore, better approximators of that exponential memory lead to improved training characteristics, by sharpening memory-retrieval.

### 3. Compact associative memory: performing memory cells for Mnemosyne

**Preliminaries.** Consider memory-vectors (patterns)  $\{\xi^\mu\}_{\mu=1}^M \subseteq \mathbb{R}^d$  (e.g. patches of the context-vector or vectors  $\nabla f(\mathbf{x}_t)$  from Sec. 1). We obtain their latent embeddings: *queries*, *keys* and *values* via learnable linear transformations  $\mathbf{W}_Q, \mathbf{W}_K \in \mathbb{R}^{N \times d}, \mathbf{W}_V \in \mathbb{R}^{d \times d}$  as follows:

$$\mathbf{q}^\mu = \mathbf{W}_Q \xi^\mu, \quad \mathbf{k}^\mu = \mathbf{W}_K \xi^\mu, \quad \mathbf{v}^\mu = \mathbf{W}_V \xi^\mu \quad (3)$$

Take a kernel (similarity measure)  $K : \mathbb{R}^N \times \mathbb{R}^N \rightarrow \mathbb{R}$ , equipped with its linear representation:  $K(\mathbf{x}, \mathbf{y}) = \mathbb{E}[\phi(\mathbf{x})^\top \phi(\mathbf{y})]$  in the  $\phi$ -transformed input space for some (usually nonlinear) mapping  $\phi : \mathbb{R}^N \rightarrow \mathbb{R}^r$ .

In the **bi-directional** setting, all the patterns are known in advance. In the **uni-directional** case, they appear in the sequential order with indices  $\mu$  playing the role of *timestamps*.

We define a *hidden state* encapsulating memory of the system of first  $t$  patterns as follows for a *discount-function*  $\lambda_t : \mathbb{R} \rightarrow \mathbb{R}$  (in the bi-directional setting we take  $t = M$ ):

$$\begin{cases} \mathbf{N}_t = \sum_{\mu=1}^t \lambda_t(\mu) \phi(\mathbf{k}^\mu) (\mathbf{v}^\mu)^\top \in \mathbb{R}^{r \times d}, \\ \Psi_t = \sum_{\mu=1}^t \lambda_t(\mu) \phi(\mathbf{k}^\mu) \in \mathbb{R}^r \end{cases} \quad (4)$$

Functions  $\lambda_t$  can be used to discount certain patterns. Even though, in principle they can be applied in the bi-directional setting, their most natural use-case is in the uni-directional one, with  $\mu$  indexing timestamps of patterns' arrivals. Here  $\lambda$  is usually applied to deprioritize older patterns.

#### 3.1. Updating hidden states and input update-rule

Note that Mnemosyne's hidden state  $\mathbf{h}_{\text{Mne}}(t) = (\mathbf{N}_t, \Psi_t)$  has size **independent** from the number of its implicitly stored patterns  $t$ . In the uni-directional case, when patterns are added,  $\mathbf{h}_{\text{Mne}}(t)$  needs to be efficiently updated on-the-fly. It is easy to see that this can be done for the *exponential discount* strategy:  $\lambda_t(\mu) = \exp(-\tau(t - \mu))$  with  $\tau \geq 0$  ( $\tau = 0$  turns off discounting). We have the following:

$$\begin{aligned} \mathbf{N}_{t+1} &= \exp(-\tau) \cdot \mathbf{N}_t + \phi(\mathbf{k}^{t+1}) (\mathbf{v}^{t+1})^\top, \\ \Psi_{t+1} &= \exp(-\tau) \cdot \Psi_t + \phi(\mathbf{k}^{t+1}) \end{aligned} \quad (5)$$

With the definition of Mnemosyne's hidden state, we can now explain how it acts on the input vectors  $\xi \in \mathbb{R}^d$ . New vector  $\xi' = \xi + \Delta\xi$  is obtained as follows, where  $\mathbf{q} = \mathbf{W}_Q \xi$ :

$$\Delta\xi = \frac{\mathbf{N}_t^\top \phi(\mathbf{q})}{\phi(\mathbf{q})^\top \Psi_t} = \sum_{\mu=1}^t \frac{\lambda_t(\mu) \phi(\mathbf{q})^\top \phi(\mathbf{k}^\mu)}{\sum_{i=1}^t \lambda_t(i) \phi(\mathbf{q})^\top \phi(\mathbf{k}^i)} \mathbf{v}^\mu \quad (6)$$

We see that  $\xi'$  can be computed in time  $O_M(1)$  and is effectively given as a convex combination of value vectors  $\mathbf{v}^\mu$ , with the coefficients proportional to the approximated kernel values, but modulated by the discount-function.

For  $\mathbf{W}_Q = \mathbf{W}_K = \mathbf{W}_V = \mathbf{I}_d$ ,  $\lambda_t \equiv 1$  and with exact kernel values  $K(\mathbf{q}, \mathbf{k}^i)$  in Eq. 6 (rather than their approximated versions  $\phi(\mathbf{q})^\top \phi(\mathbf{k}^i)$ ), dynamical systems defined by Eq. 6 become effectively Hopfield networks and, as energy-based models with energies given as  $E(\xi; \{\xi^\mu\}_{\mu=1}^t) = -\sum_{\mu=1}^t K(\xi, \xi^\mu)$ , retrieve memory-vectors upon energy-minimization-driven convergence (Ramsauer et al., 2020). The quality of the memory retrieval heavily depends on the kernel used with the softmax-kernel  $K(\mathbf{x}, \mathbf{y}) \stackrel{\text{def}}{=} \exp(\mathbf{x}^\top \mathbf{y})$  providing particularly strong theoretical results.

For arbitrary  $\mathbf{W}_Q, \mathbf{W}_K, \mathbf{W}_V$ , but still with  $\lambda_t \equiv 1$  and exact kernel values, Eq. 6 turns into regular Transformers' attention. Upon replacement of the exact kernel values with the approximate ones, Performer model is recovered.

We think about Eq. 6 as a *generalized* (since it uses  $\lambda_t$ ) *compact* (since it provides efficient hidden state and input update-rules via linearized kernels from Performers) *associative memory* model (CAM) (as opposed to the regular associate memory model from Hopfield networks). CAM can be applied flexibly: either as a part of larger Transformer-stacks (usually in the bi-directional setting, see: Sec. 5.2) or a light-memory on its own, replacing LSTM memory-cells (in the uni-directional setting, see: Sec. 5.1).

#### 3.2. Kernel-linearizations for Mnemosyne's memory

We tested different transformations  $\phi$  and discovered that those leading to most accurate approximation of the softmax-kernel lead to most effective memory mechanisms (see: Sec. 5.1). Our starting variant is the so-called *FAVOR+* mechanism from Choromanski et al. (2021), given as follows for  $\Gamma(\mathbf{z}, r) \stackrel{\text{def}}{=} \frac{1}{\sqrt{r}} \exp(-\frac{\|\mathbf{z}\|^2}{2})$  and  $\omega_1, \dots, \omega_r \sim \mathcal{N}(0, \mathbf{I}_N)$ :

$$\phi_{F+}(\mathbf{z}) = \Gamma(\mathbf{z}, r) (\exp(\omega_1^\top \mathbf{z}), \dots, \exp(\omega_r^\top \mathbf{z}))^\top \quad (7)$$

Random vectors  $\omega_1, \dots, \omega_r$  form a block-orthogonal ensemble (see: (Choromanski et al., 2021)). We applied also its improvement relying on the so-called *hyperbolic cosine random features*, where  $\prod$  is the concatenation operator:

$$\phi_{HF+}(\mathbf{z}) = \Gamma(\mathbf{z}, r) \prod_{i=1}^{\frac{r}{2}} (\exp(\omega_i^\top \mathbf{z}), \exp(-\omega_i^\top \mathbf{z}))^\top \quad (8)$$

Both randomized transformations provide **unbiased** estimation of the softmax-kernel, yet the latter one (that can be cast as modified  $\phi_{F+}$  via the antithetic Monte Carlo trick) has provably lower approximation variance.

### 3.2.1. THE CURIOUS CASE OF LINEARIZATION WITH BOUNDED FEATURES

The last variant for the efficient estimation of the softmax-kernel we applied, is a very recent mechanism *FAVOR++* from (Likhosherstov et al., 2022), given as:

$$\phi_{F++}(\mathbf{z}) = \frac{D}{\sqrt{r}} \prod_{i=1}^r \exp(-\widehat{A}\|\omega_i\|_2^2 + B\omega_i^\top \mathbf{z} + C\|\mathbf{z}\|^2)^\top,$$

where we have:  $\widehat{A} = -A$ ,  $B = \sqrt{1 + 4\widehat{A}}$ ,  $C = -\frac{1}{2}$ ,  $D = (1 + 4\widehat{A})^{\frac{N}{4}}$ ,  $A = 1 - \frac{1}{\rho}$  and  $\rho \in (0, 1)$  is a free parameter. As opposed to the previous variants, mechanism  $\phi_{F++}(\mathbf{z})$  provides an estimation via **bounded** random variables (since  $\widehat{A} > 0$ ), leading to stronger concentration results (beyond second moment) and still unbiased approximation.

The optimal choice of  $\rho$  depends on the kernel inputs. The formula for  $\rho$  optimizing the variance of the entire kernel matrix estimation  $\mathcal{K} = [\mathbf{K}(\mathbf{q}^i, \mathbf{k}^j)]_{i,j=1,\dots,M}$  induced by the softmax-kernel  $\mathbf{K}$  (in the bi-directional case) is not tractable. However choosing  $\rho$  by optimizing certain derivative of the variance-objective was showed to work well in several Transformer-applications (Likhosherstov et al., 2022):

$$\rho^* = \frac{\sqrt{(2\gamma + N)^2 + 8N\gamma} - 2\gamma - N}{4\gamma} \quad (9)$$

for  $\gamma = \frac{1}{M^2} \sum_{i=1}^M \sum_{j=1}^M \|\mathbf{q}^i + \mathbf{k}^j\|^2$ . Since  $\gamma$  can be rewritten as:  $\gamma = \frac{1}{M^2} (\sum_{i=1}^M \|\mathbf{q}^i\|_2^2 + \sum_{j=1}^M \|\mathbf{k}^j\|_2^2 + 2\mathbf{q}^\top \mathbf{k})$  for  $\mathbf{q} = \sum_{i=1}^M \mathbf{q}^i$  and  $\mathbf{k} = \sum_{j=1}^M \mathbf{k}^j$ , computing  $\rho^*$  in the bi-directional setting can be clearly done in time linear in  $M$  as a **one-time** procedure. Then the computation of  $\mathbf{h}_{\text{Mne}}(M)$  follows. Compute-time per memory-vector remains  $O_M(1)$ .

In the uni-directional case, we have:  $\gamma_t = \frac{1}{t} \sum_{j=1}^t \|\mathbf{q}^t + \mathbf{k}^j\|^2 = \frac{1}{t} (\|\mathbf{q}^t\|_2^2 + \sum_{j=1}^t \|\mathbf{k}^j\|_2^2 + 2(\mathbf{q}^t)^\top \mathbf{k}(t))$ , where  $\mathbf{k}(t) = \sum_{j=1}^t \mathbf{k}^j$  for  $t = 1, \dots, M$ . Instead of one  $\gamma$ , we now have  $M$  values  $\gamma_t$  since not all memories are known at once. We can still achieve  $O_1(M)$  compute-time per  $\gamma_t$ , repeating the trick from the bi-directional case, but that would need to be followed by the re-computation of  $\phi(\mathbf{k}^\mu)$  (with new  $\rho$ -parameter) for  $\mu = 1, \dots, t$  which of course is not possible since vectors  $\{\mathbf{k}\}_{\mu=1}^t$  are not explicitly stored (and for a good reason - computational benefits), see: Eq. 4.

**Thickening Mnemosyne’s memory:** To obtain efficient uni-directional Mnemosyne’s memory cell also for the  $\phi_{F++}$ -mechanism, we propose to “thicken” in that setting the hidden state from Eq. 4, replacing  $\mathbf{h}_{\text{Mne}}(t) = (\mathbf{N}_t, \Psi_t)$  with  $\mathbf{H}_{\text{Mne}}(t) = (\{\mathbf{N}_t^\rho\}_{\rho \in \Omega}, \{\Psi_t^\rho\}_{\rho \in \Omega}, \Sigma_t, \Lambda_t)$ , where we have:  $\Sigma_t = \sum_{j=1}^t \mathbf{k}^j$ ,  $\Lambda_t = \sum_{j=1}^t \|\mathbf{k}^j\|_2^2$  and furthermore:  $\mathbf{N}_t^\rho, \Psi_t^\rho$  correspond to versions of  $\mathbf{N}_t$  and  $\Psi_t$  respectively, using parameter  $\rho$  to define mapping  $\phi$ . The set  $\Omega$  is obtained by discretizing interval  $(0, 1)$  into a fixed number of

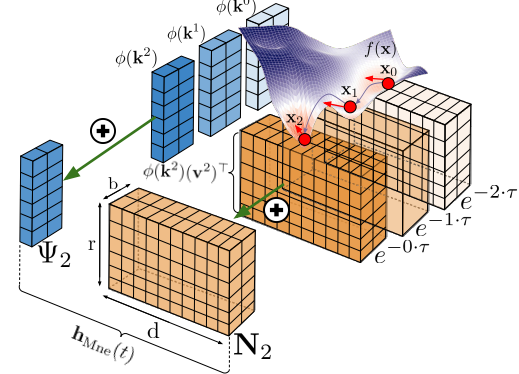


Figure 1. Pictorial description of Mnemosyne in the uni-directional (causal) setting (patterns are counted from  $t = 0$ ). Parameter  $b$  denotes batch size. More recent memories (cubes of more vivid colors) are prioritized through the exponential discount.

chunks  $c$  (and effectively quantizes  $\rho \in (0, 1)$ ). The strategy is now clear: when the new pattern comes, we first update the entire thickened state, and then compute  $\rho^*$ . We finalize by finding  $\rho \in \Omega$  closest to  $\rho^*$  to transform an input and using for that the “slice” of the hidden state corresponding to  $\rho$ . We see that all these operations can be made efficiently with only  $c$ -multiplicative term (**independent** from the number of patterns  $M$ ) in space and time complexity.

FAVOR++ mechanism, as FAVOR+, can also be adapted to its hyperbolic cosine variant. In practice FAVOR+ mechanism worked similarly to FAVOR++, yet the proper adaptation of the latter one was important, since (see: Sec. 4), this variant provides strongest theoretical guarantees for the capacity of the entire compact associative memory model.

### 3.3. Mnemosyne’s memory vs RNNs & Transformers

In the uni-directional setting, presented Mnemosyne’s memory model in many ways resembles more classic RNN/LSTM memory-cell (Hochreiter & Schmidhuber, 1997), with the residual-update mechanism from Eq. 6 as a particular gating technique and compact hidden state  $\mathbf{h}_{\text{Mne}}$  of size independent from the history length (which is not the case for regular Transformers!). The mechanism is much simpler though than its LSTM-analogue (see: Fig. 1) and is based on a fundamentally different approach leveraging energy-based models which, as we show in Sec. 5.1, plays crucial role in training. We have also tried to use regular Transformer attention blocks to encode memory, but this approach turned out not very practical due to the quadratic space/time complexity of the regular attention mechanism and consequently, more complicated memory-update rules based on fixed length history caching (see: Sec. 5.1).

## 4. The theory of Mnemosyne’s memory

In this section, we analyze Mnemosyne’s compact associative memory (CAM) from the theoretical point of view. We show that, as its regular non-compact counterpart, it is

capable of storing patterns, but (as opposed to the former) in the implicit manner. We start by providing a concise introduction to associative memory models as "analytical" (rather than combinatorial) energy-based nearest-neighbor search systems. We then present our main result (Theorem 4.4) stating that "on average" CAMs can restore exponentially many (in space dimensionality) number of patterns, provided that they are spread "well enough". To the best of our knowledge, this is the first result of this type.

#### 4.1. Regular Exponential Associative Memory

As in several other papers analyzing associative memory from the theoretical point of view, we consider feature vectors taken from the set  $\{-1, +1\}^N$ . We denote by  $\{\xi^\mu\}_{\mu=1}^M$  the set of all the memory-vectors to be stored. For the given input  $\xi$ , in the regular exponential associative memory model, the energy of the system is defined as:

$$E_{\text{reg}}(\xi; \xi^1, \dots, \xi^M) = - \sum_{\mu=1}^M \exp(\xi^\top \xi^\mu). \quad (10)$$

The dynamical system defining the interactions with the associative memory and whose goal is to retrieve the relevant memory for the given input vector  $\sigma \in \{-1, +1\}^N$  (its nearest neighbor in  $\{\xi\}_{\mu=1}^M$ ) has the following form:

$$\sigma \rightarrow T_{i_1}(\sigma) \rightarrow T_{i_2}(T_{i_1}(\sigma)) \rightarrow \dots, \quad (11)$$

for the initial point  $\sigma$ , where  $i_1, i_2, \dots$  are chosen independently at random and  $T_j : \{-1, +1\}^N \rightarrow \{-1, +1\}^N$  only updates the  $j$ th entry of its input as follows (for  $\xi[j; x]$  denoting vector  $\xi$ , but with its  $j$ th dimension equal to  $x$ ):

$$T_j(\xi)[j] = \text{sgn}[E_{\text{reg}}(\xi[j; -1]; \xi^1, \dots, \xi^M) - E_{\text{reg}}(\xi[j; 1]; \xi^1, \dots, \xi^M)] \quad (12)$$

Thus at every step, a random dimension of the input vector is chosen and its value is flipped if that operation decreases the energy of the system.

**Definition 4.1** (the capacity of the associative models). We say that the model described above stores memories  $\{\xi^\mu\}_{\mu=1}^M$  if there exists  $\rho \in (0, \frac{1}{2})$  such that the following holds for any  $j$  and  $\hat{\xi}^\mu$  taken from the Hamming ball  $\mathcal{B}(\xi^\mu, \rho N)$  centered in  $\xi^\mu$  and of Hamming radius  $\rho N$ :

$$T_j(\hat{\xi}^\mu)[j] = \xi_j^\mu \quad (13)$$

It was proven in Demircigil et al. (2017) that if the memories are chosen uniformly and independently at random from  $\{-1, +1\}^N$ , then with probability approaching 1 as  $N \rightarrow \infty$  the model stores all the memories as long as the memory-set is not too large. Most importantly, the upper bound on the memories-set size is exponential in  $N$ .

**Remark 4.2.** Despite the exponential capacity of the model, all its memories need to be explicitly stored (in order to compute the energy-function) and the compute time is proportional to their number. Thus for large number of memories, the space and time complexity makes the retrieval process infeasible in practice.

#### 4.2. Mnemosyne's Compact Associative Memory

We denote by  $\omega_1, \omega_2, \dots, \omega_r$  samples chosen independently from the multivariate Gaussian distribution  $\mathcal{N}(0, \mathbf{I}_N)$  and define the energy of the system as follows:

$$E_{\text{rand}}(\xi; \xi^1, \dots, \xi^M) = \phi_{F++}(\xi)^\top \mathbf{M}(\xi^1, \dots, \xi^M), \quad (14)$$

where  $\mathbf{M}$  is given below (for  $\phi_{F++}$ , as in Sec. 3.2.1)

$$\mathbf{M}(\xi^1, \dots, \xi^M) = - \sum_{\mu=1}^M \phi_{F++}(\xi^\mu) \quad (15)$$

We refer to the number of random projection vectors  $\omega$  as the *number of random features*.

Equipped with this new energy function, we define the corresponding dynamical system in the same way as for the regular associative memory model.

**Remark 4.3.** Note that calculating our energy  $E_{\text{rand}}$  can be now done efficiently in time  $O(r)$ , once vector  $\mathbf{M}$  is computed (thus independently from the number of implicitly stored memories). In the online/streaming setting, when the memories come one by one, updating vector  $\mathbf{M}$  can be conducted in time  $O(Nr)$  per query.

#### 4.3. The capacity of the Mnemosyne's memory

We are ready to present our main theoretical result. We assume the kernel linearization setting from Sec. 3.2.1 and use the corresponding notation.

**Theorem 4.4** (storage of compact associative memories). Denote by  $\xi^1, \dots, \xi^M \in \{-1, +1\}^N$  the memory-vectors. Assume that the Hamming distance between any two memory-vectors is at least  $\tau N$  for some  $\tau > 0$ . Take some  $0 < \rho < \frac{\tau}{2}$ . Then the following is true for any memory-vector  $\xi^l$  for  $l = 1, \dots, M$  and any input  $\hat{\xi}^l \in \mathcal{B}(\xi^l, \rho N)$  as long as  $M \leq \exp(2N(\tau - 2\rho)) \frac{1 - e^{-2}}{2e^2}$ : the expected change of the energy of the compact associative memory system  $\Delta(E_{\text{rand}})$  associated with flipping the value of the dimension of  $\hat{\xi}^l$  is positive if that operation increases the distance from its close neighbor  $\xi^l$  and is negative otherwise. Furthermore, the variance of  $\Delta(E_{\text{rand}})$  is of the form:

$$\text{Var}(\Delta(E_{\text{rand}})) = \frac{1}{r} (V_1 + V_2 - 2V_3 - V_4 - V_5 + 2V_6) \quad (16)$$

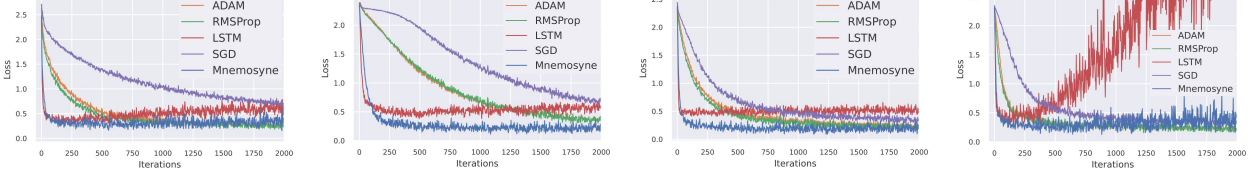


Figure 2. Validation loss curves when training MLP with Mnemosyne compared to other methods for MNIST image classification. Optimization curves for 4 different MLP architectures in this order: (1 layer, 20 hidden dim, sigmoid activation), (2 layers, 20 hidden dim, sigmoid activation), (1 layer, 40 hidden dim, sigmoid activation), (1 layer, 20 hidden dim, relu activation) are shown.

where:

$$\begin{aligned}
V_1 &= \sum_{\mu_1, \mu_2 \in \{1, \dots, M\}} \Psi(\xi^{\mu_1} + \xi^{\mu_2} + 2\tilde{\xi}^l) \\
V_2 &= \sum_{\mu_1, \mu_2 \in \{1, \dots, M\}} \Psi(\xi^{\mu_1} + \xi^{\mu_2} + 2\tilde{\xi}^l) \\
V_3 &= \sum_{\mu_1, \mu_2 \in \{1, \dots, M\}} \Psi(\xi^{\mu_1} + \xi^{\mu_2} + \tilde{\xi}^l + \tilde{\xi}^l) \\
V_4 &= \sum_{\mu_1, \mu_2 \in \{1, \dots, M\}} \exp((\xi^{\mu_1})^\top \tilde{\xi}^l) \exp((\xi^{\mu_2})^\top \tilde{\xi}^l) \\
V_5 &= \sum_{\mu_1, \mu_2 \in \{1, \dots, M\}} \exp((\xi^{\mu_1})^\top \tilde{\xi}^l) \exp((\xi^{\mu_2})^\top \tilde{\xi}^l) \\
V_6 &= \sum_{\mu_1, \mu_2 \in \{1, \dots, M\}} \exp((\xi^{\mu_1})^\top \tilde{\xi}^l) \exp((\xi^{\mu_2})^\top \tilde{\xi}^l)
\end{aligned} \quad (17)$$

for  $\tilde{\xi}^l$  denoting  $\hat{\xi}^l$  with one of its dimensions flipped and:

$$\Psi(\mathbf{x}) \stackrel{\text{def}}{=} D^4 \exp(-2N)(1 + 8\hat{A})^{-\frac{N}{2}} \exp\left(\frac{B^2}{2(1 - 8\hat{A})} \|\mathbf{x}\|^2\right) \quad (18)$$

**Remark 4.5.** Theorem 4.4 says that the expected value of the change of the energy of the system has the correct sign even if the number of stored patterns is exponential in their dimensionality, provided that the patterns are well separated. Furthermore, not surprisingly, the variance of the estimation is inversely proportional to the number of random features  $r$ . By the analogous argument as the one provided in Sec. A.1 in the proof of Theorem 4.4, a similar statement for the mechanism applying  $\phi_{F+}$  can be derived. However  $\phi_{F++}$  provides **the smallest** variance among all competitors as the most accurate currently known mechanism for the unbiased softmax-kernel approximation.

## 5. Experiments

### 5.1. Causal Mnemosyne for ML Training

**Preliminaries:** In this setting, Mnemosyne’s optimizer  $g_{\theta_2}^{\text{hist}}$  is used to encode the parameter update-rule for training NN architectures. At each timestep  $t$ , gradient  $\nabla f(\mathbf{x}_t)$  is input to the optimizer, for each coordinate independently. The gradient is pre-processed as proposed in Andrychowicz et al. (2016) and given to 2 compact Mnemosyne’s memory cells sequentially. The Mnemosyne’s memory cell interfaces with the rest of the system similarly to any RNN-cell. Each cell uses exponential discount factor  $\tau = 0.1$ ,  $r = 16$  random

projections, 16 hidden dimensions and 1 attention head. The memory cell output is fed to a fully connected layer which returns the update to be applied to the NN parameters of the optimizee.

**Training details:** We refer to training optimizer’s parameters  $\theta_2$  as *meta-training* to distinguish from the optimizee NN training. Mnemosyne’s optimizer is meta-trained only on a single ML task: MLP MNIST classifier. The optimizee MLP has  $l = 1$  hidden layer of size  $h = 20$  and uses sigmoid activation function. The optimizee task is to train MLP for 100 steps on batches of 128 image-class examples.

**Hybrid loss function to improve generalization:** To promote generalization to new tasks, we use the random-scaling trick proposed by Lv et al. (2017). Mnemosyne’s optimizer is meta-trained by gradient descent using Adam optimizer with learning rate  $\eta = 3e-4$  to minimize a combination of two loss functions. The first is the task loss given by the sum of optimizee losses in a truncated roll-out of 5 MLP training steps. The other one is an imitation loss given by the mean squared error between Mnemosyne’s updates and expert-optimizer (Adam) updates for same inputs. Importantly, this imitation loss is different from the one proposed in Chen et al. (2020) which uses off-policy expert roll-outs for imitation. In our case, we provide expert supervision for the on-policy updates. This mitigates the problem of divergence from expert’s trajectory, often observed in behaviour cloning. Our imitation loss acts as a regularizer which prevents Mnemosyne’s optimizer from over-fitting on the optimizee task that it is trained on.

Our optimizer model has minimal input feature engineering and our meta-training setup is significantly simpler than those considered in the literature (Metz et al., 2020; Chen et al., 2020; Lv et al., 2017; Wichrowska et al., 2017). Even so, we can successfully apply Mnemosyne’s optimizer to a variety of tasks due to its efficient memory mechanism. Furthermore, Mnemosyne’s memory cells can be easily combined with any of the existing L2L methods that use LSTMs for memory-encoding.

**Results:** After meta-training, Mnemosyne’s optimizer was tested on NN training tasks with different NN architectures and datasets. Recall that Mnemosyne only saw one ML task of MLP classifier training on MNIST dataset for 100 steps

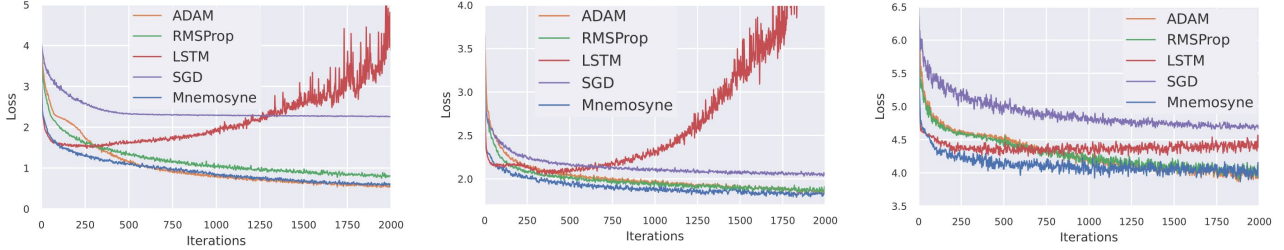


Figure 3. Validation loss curves while training Vision Transformer with Mnemosyne compared to other methods for image classification on 3 different datasets, **top**: MNIST, **middle**: CIFAR10 and **bottom**: CIFAR100 are shown.

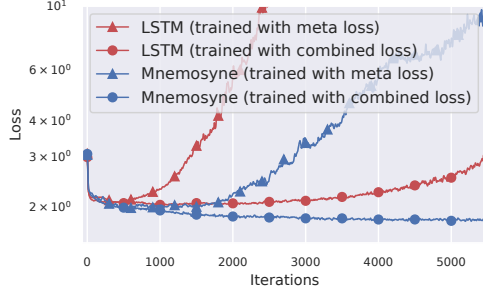


Figure 4. Impact of training the optimizer with combined meta loss and imitation loss can be seen in generalization to a long horizon rollout. All variants were trained only on length 100 rollouts.

during meta-training. Fig. 2 shows that Mnemosyne can optimize MLPs with different NN architectures and activation functions on MNIST image classifier training. Note that, Mnemosyne converges significantly faster than popular analytical optimizers, RMSprop and Adam while retaining similar asymptotic performance. Mnemosyne can train NNs for long horizons of thousands of steps while baseline LSTM optimizer (Andrychowicz et al., 2016) struggles to minimize classification loss beyond a few hundred steps.

**Transformers:** Mnemosyne was also tested on the task of training vision transformers (ViTs) (Dosovitskiy et al., 2021) which have significantly different architectures than MLPs. Considered ViT has 3 attention and MLP layers of size 16 and 2 heads. Training curves for image classification with ViTs on different datasets (MNIST, CIFAR10, CIFAR100) are shown in Fig. 3. Here, as before, Mnemosyne’s optimizer is faster than standard analytical optimizers and more stable than LSTM optimizer.

The stability of Mnemosyne’s optimizer is also owed to the on-policy imitation loss for meta-training. Fig. 4 shows the benefit of using expert imitation-loss for long-horizon stability of the Mnemosyne’s optimizer.

Our results on training Transformers with Mnemosyne naturally lead to the question of the role that Transformer-based optimizers can play in training Transformers architectures. It is well known that Transformer training requires nontrivial optimization techniques (Liu et al., 2020), e.g. learning rate schedulers (for that reason SGD was replaced with Adam in Transformer-training). Furthermore, for larger architectures training is slow, often prohibitively (unless the model

is trimmed down, for instance by replacing long-range attention modeling with local attention of the controllable attention radius). Attention-based optimizers can potentially address this problem, since they improve convergence (and thus effectively reduce training time) even if meta-trained on much simpler tasks that do not involve attention-based models, as we show in Fig. 3.

**Ablation studies:** We have tried to use regular Transformer attention-based decoder blocks to encode memory. For applying regular attention to online optimizer autoregressively, a limited-length cache of historical gradients has to be maintained. A self-attention map over the history sequence is generated and used to encode memory. Fig. 5 (left) shows the meta-training curves for regular attention optimizers with different history cache lengths. As we increase the cache length, the performance improves and the memory requirement scales quadratically. Due to this limitation, we could not implement a regular attention based optimizer with cache length more than 100. On the other hand, Performer’s memory cell can attend to theoretically unbounded history and the finally out-performs regular attention variants with fixed memory requirement.

Fig. 5 (middle) compares the performance of Mnemosyne optimizer with FAVOR+ and FAVOR++ mechanisms explained in Sec. 3. FAVOR++ mechanism provides strongest theoretical guarantees for the capacity of the associative memory model but FAVOR+ performs comparably in practice. Due to the simpler implementation of FAVOR+, we use it for all experiments with Mnemosyne’s optimizer.

In Fig. 5, we compare the performance of Mnemosyne for different maps  $\phi$ . FAVOR++ mechanism leads initially to faster convergence, but asymptotically performs similarly as the FAVOR+ variant (middle). Optimizers with both regular positive and hyperbolic random features kernel learn similarly, but the latter has much lower variance (right).

## 5.2. Spatial Mnemosyne for initializing MPC optimizers

**Preliminaries:** We applied Mnemosyne with bidirectional spatial attention for learning trajectory optimizers to be used for wheeled robot navigation in complex, photo-realistic simulated environments. The robot uses vision sensors for

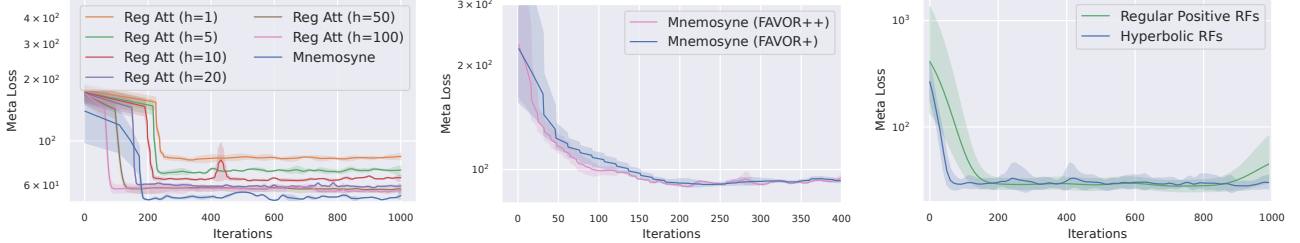


Figure 5. Ablation Studies. **Left:** Comparison of Mnemosyne linear memory with regular attention memory blocks with different history cache lengths ( $h$ ). **Middle:** Meta-training curves of Mnemosyne optimizer with FAVOR+ and FAVOR++ mechanism. **Right:** Meta-training curves of Mnemosyne optimizer with different kernel transformation functions.

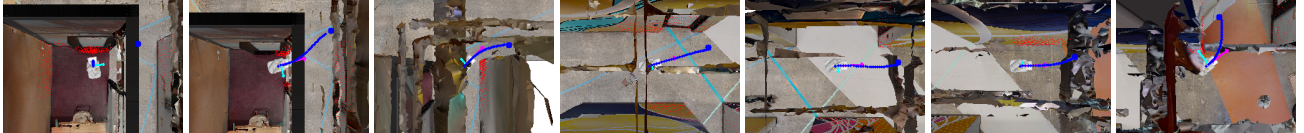


Figure 6. Navigation in a photo-realistic environment with MPC policy using Mnemosyne optimizer for initializing SQP solver.

observing an occupancy grid of the environment and navigates using linear and angular velocity control. Navigation in challenging environments requires efficient high-speed robot control. Model Predictive Control (MPC) presents an efficient approach to the navigation problem, provided that the motion-planning with the environment model can be carried out within computational real-time limits (Xiao et al., 2022). Motion planning with efficient trajectory optimizers such as iterative Linear Quadratic Regulator (iLQR) (Li & Todorov, 2004) is one way to implement MPC. However, in challenging layouts with narrow corridors and doors and with conservative safety and collision avoidance constraints, iLQR struggles to converge to the optimal trajectory. Sequential Quadratic Programming (SQP) (Singh et al., 2021) is often a more robust optimizer that can handle difficult non-linear constraints. However, SQP is significantly, sometimes  $\sim 10$  times, slower than iLQR and hence cannot be deployed in real-time settings. Deep Learning models have been shown to accelerate SQP by warm starting the optimization process (Ichnowski et al., 2020). We learn Mnemosyne’s optimizer to imitate SQP behaviour and initialize it with an approximately optimal trajectory as a starting point from which SQP refines to an optimized and feasible trajectory.

**Training details:** Mnemosyne’s optimizer,  $g_{\theta_1}^{init}$ , receives current robot pose  $p_r$ , a goal pose  $p_g$  and a visual occupancy grid as the context,  $\mathbf{c}$ . The occupancy grid is processed by an image encoder module, a ViT where the attention mechanism is approximated by bidirectional Mnemosyne memory. As in a ViT, the occupancy grid is first pre-processed by a convolution layer and then flattened to a sequence. Each element (token) of the sequence corresponds to a different  $5 \times 5$  patch of the original frame which is then enriched with positional encoding. The pre-processed input is then fed to 3 Mnemosyne attention and MLP layers of hidden dimension 64. The final embedding of one of the tokens is chosen as a latent representation of the occupancy grid,  $l_{oc}$ .

$p_r$ ,  $p_g$  and  $l_{oc}$  are concatenated and processed by an MLP which outputs the predicted action trajectory,  $\mathbf{x}_0$ .

An offline dataset of SQP optimization examples is collected by running MPC navigation agent in 2787 different environments. Each navigation run has 180 steps on average. For each MPC step, one instance of trajectory optimization with SQP was run and a pair of input context  $\mathbf{c}$  and the final optimal trajectory  $\mathbf{x}_T$  was recorded. A total of  $\sim 500,000$  training examples were collected. Mnemosyne’s optimizer was trained with supervised learning on the SQP dataset by minimizing mean squared error between the SQP optimal trajectories and the predicted trajectories.

**Results:** After training, the predicted trajectory from Mnemosyne was used to initialize SQP optimization. Without Mnemosyne initialization, SQP optimization was capped at maximum 10 iterations. It took on average 4.78 iterations and 0.12sec for the SQP solution to complete. With Mnemosyne initialization, SQP is only run for 1 iteration to reach the optimal trajectory. SQP generates a trajectory that satisfies kinematic, dynamic and safety constraints for the robot which transformer alone e.g. Brohan et al. (2022) cannot natively guarantee. This reduces the optimization time by more than half to 0.048sec on average which is under real-time constraint. It includes 0.011sec for Mnemosyne inference and the rest for SQP iteration. A sequence of snapshots during navigation with Mnemosyne-SQP optimizer in a sample environment is shown in Fig. 6. Videos of simulated robot navigation can be seen on our project page.

## 6. Conclusion

We proposed a new learning to learn (L2L) paradigm based on scalable low-rank implicit attention memory cells, previously successfully applied in Performers architectures (Choromanski et al., 2021). Our resulting system, Mnemosyne, takes the best from both the worlds: (a) com-

pact representation of the memory (as in RNNs), critical for efficient computation, (b) the expressiveness provided by associative memory and attention mechanism which is behind the success of Transformers. Furthermore, we have provided extensive empirical evaluation of our system, ranging from regular L2L tasks (training neural network classifiers) to learning initializers for MPC optimizers in Robotics. These results include training Transformers with Transformers, meta-trained on tasks involving simpler attention-free architectures. Our results are confirmed by the theoretical analysis. To the best of our knowledge, we are the first to provide strong capacity results for compact associative memory mechanisms, an algorithmic core of Mnemosyne. Finally, we believe that this paper can catalyze a research on the applications of learnable attention-based optimizers in the notoriously difficult problem of Transformers training.

## References

- Alet, F., Lozano-Pérez, T., and Kaelbling, L. P. Modular meta-learning. In *2nd Annual Conference on Robot Learning, CoRL 2018, Zürich, Switzerland, 29-31 October 2018, Proceedings*, volume 87 of *Proceedings of Machine Learning Research*, pp. 856–868. PMLR, 2018. URL <http://proceedings.mlr.press/v87/alet18a.html>.
- Andrychowicz, M., Denil, M., Colmenarejo, S. G., Hoffman, M. W., Pfau, D., Schaul, T., and de Freitas, N. Learning to learn by gradient descent by gradient descent. In Lee, D. D., Sugiyama, M., von Luxburg, U., Guyon, I., and Garnett, R. (eds.), *Advances in Neural Information Processing Systems 29: Annual Conference on Neural Information Processing Systems 2016, December 5-10, 2016, Barcelona, Spain*, pp. 3981–3989, 2016.
- Bengio, S., Bengio, Y., Cloutier, J., and Gecsei, J. On the optimization of a synaptic learning rule. In *Conference on Optimality in Biological and Artificial Networks*, 1992.
- Bengio, S., Bengio, Y., Cloutier, J., and Gecsei, J. On the search for new learning rules for anns. In *Neural Processing Letters*, pp. 26–30, 1995.
- Berseth, G., Zhang, Z., Zhang, G., Finn, C., and Levine, S. Comps: Continual meta policy search. In *The Tenth International Conference on Learning Representations, ICLR 2022, Virtual Event, April 25-29, 2022*. OpenReview.net, 2022. URL <https://openreview.net/forum?id=PVJ6j87g0Hz>.
- Brohan, A., Brown, N., Carbalal, J., Chebotar, Y., Dabis, J., Finn, C., Gopalakrishnan, K., Hausman, K., Herzog, A., Hsu, J., et al. Rt-1: Robotics transformer for real-world control at scale. *arXiv preprint arXiv:2212.06817*, 2022.
- Brown, T. B., Mann, B., Ryder, N., Subbiah, M., Kaplan, J., Dhariwal, P., Neelakantan, A., Shyam, P., Sastry, G., Askell, A., Agarwal, S., Herbert-Voss, A., Krueger, G., Henighan, T., Child, R., Ramesh, A., Ziegler, D. M., Wu, J., Winter, C., Hesse, C., Chen, M., Sigler, E., Litwin, M., Gray, S., Chess, B., Clark, J., Berner, C., McCandlish, S., Radford, A., Sutskever, I., and Amodei, D. Language models are few-shot learners. In Larochelle, H., Ranzato, M., Hadsell, R., Balcan, M., and Lin, H. (eds.), *Advances in Neural Information Processing Systems 33: Annual Conference on Neural Information Processing Systems 2020, NeurIPS 2020, December 6-12, 2020, virtual*, 2020.
- Cao, Y., Chen, T., Wang, Z., and Shen, Y. Learning to optimize in swarms. In Wallach, H. M., Larochelle, H., Beygelzimer, A., d’Alché-Buc, F., Fox, E. B., and Garnett, R. (eds.), *Advances in Neural Information Processing Systems 32: Annual Conference on Neural Information Processing Systems 2019, NeurIPS 2019, December 8-14, 2019, Vancouver, BC, Canada*, pp. 15018–15028, 2019.
- Chen, M. X., Firat, O., Bapna, A., Johnson, M., Macherey, W., Foster, G. F., Jones, L., Schuster, M., Shazeer, N., Parmar, N., Vaswani, A., Uszkoreit, J., Kaiser, L., Chen, Z., Wu, Y., and Hughes, M. The best of both worlds: Combining recent advances in neural machine translation. In Gurevych, I. and Miyao, Y. (eds.), *Proceedings of the 56th Annual Meeting of the Association for Computational Linguistics, ACL 2018, Melbourne, Australia, July 15-20, 2018, Volume 1: Long Papers*, pp. 76–86. Association for Computational Linguistics, 2018. doi: 10.18653/v1/P18-1008. URL <https://aclanthology.org/P18-1008/>.
- Chen, T., Zhang, W., Zhou, J., Chang, S., Liu, S., Amini, L., and Wang, Z. Training stronger baselines for learning to optimize. In Larochelle, H., Ranzato, M., Hadsell, R., Balcan, M., and Lin, H. (eds.), *Advances in Neural Information Processing Systems 33: Annual Conference on Neural Information Processing Systems 2020, NeurIPS 2020, December 6-12, 2020, virtual*, 2020.
- Chen, T., Chen, X., Chen, W., Heaton, H., Liu, J., Wang, Z., and Yin, W. Learning to optimize: A primer and A benchmark. *CoRR*, abs/2103.12828, 2021. URL <https://arxiv.org/abs/2103.12828>.
- Chen, Y., Hoffman, M. W., Colmenarejo, S. G., Denil, M., Lillicrap, T. P., and de Freitas, N. Learning to learn for global optimization of black box functions. *CoRR*, abs/1611.03824, 2016. URL <http://arxiv.org/abs/1611.03824>.
- Chen, Y., Song, X., Lee, C., Wang, Z., Zhang, Q., Doohan, D., Kawakami, K., Kochanski, G., Doucet, A., Ranzato, M., Perel, S., and de Freitas, N. Towards learn-

- ing universal hyperparameter optimizers with transformers. *CoRR*, abs/2205.13320, 2022. doi: 10.48550/arXiv.2205.13320. URL <https://doi.org/10.48550/arXiv.2205.13320>.
- Choromanski, K., Lin, H., Chen, H., Zhang, T., Sehanobish, A., Likhosherstov, V., Parker-Holder, J., Sarlós, T., Weller, A., and Weingarten, T. From block-Toeplitz matrices to differential equations on graphs: towards a general theory for scalable masked transformers. In Chaudhuri, K., Jegelka, S., Song, L., Szepesvári, C., Niu, G., and Sabato, S. (eds.), *International Conference on Machine Learning, ICML 2022, 17-23 July 2022, Baltimore, Maryland, USA*, volume 162 of *Proceedings of Machine Learning Research*, pp. 3962–3983. PMLR, 2022. URL <https://proceedings.mlr.press/v162/choromanski22a.html>.
- Choromanski, K. M., Likhosherstov, V., Dohan, D., Song, X., Gane, A., Sarlós, T., Hawkins, P., Davis, J. Q., Mohiuddin, A., Kaiser, L., Belanger, D. B., Colwell, L. J., and Weller, A. Rethinking attention with performers. In *9th International Conference on Learning Representations, ICLR 2021, Virtual Event, Austria, May 3-7, 2021*. OpenReview.net, 2021. URL <https://openreview.net/forum?id=Ua6zuk0WRH>.
- Chowdhery, A., Narang, S., Devlin, J., Bosma, M., Mishra, G., Roberts, A., Barham, P., Chung, H. W., Sutton, C., Gehrmann, S., Schuh, P., Shi, K., Tsvyashchenko, S., Maynez, J., Rao, A., Barnes, P., Tay, Y., Shazeer, N., Prabhakaran, V., Reif, E., Du, N., Hutchinson, B., Pope, R., Bradbury, J., Austin, J., Isard, M., Gur-Ari, G., Yin, P., Duke, T., Levskaya, A., Ghemawat, S., Dev, S., Michalewski, H., Garcia, X., Misra, V., Robinson, K., Fedus, L., Zhou, D., Ippolito, D., Luan, D., Lim, H., Zoph, B., Spiridonov, A., Sepassi, R., Dohan, D., Agrawal, S., Omernick, M., Dai, A. M., Pillai, T. S., Pelлат, M., Lewkowycz, A., Moreira, E., Child, R., Polozov, O., Lee, K., Zhou, Z., Wang, X., Saeta, B., Diaz, M., Firat, O., Catasta, M., Wei, J., Meier-Hellstern, K., Eck, D., Dean, J., Petrov, S., and Fiedel, N. Palm: Scaling language modeling with pathways. *CoRR*, abs/2204.02311, 2022. doi: 10.48550/arXiv.2204.02311. URL <https://doi.org/10.48550/arXiv.2204.02311>.
- Chowdhury, S. P., Solomou, A., Dubey, A., and Sachan, M. On learning the transformer kernel. *Transactions of Machine Learning Research*, 2022. URL <https://arxiv.org/abs/2110.08323>.
- Demircigil, M., Heusel, J., Löwe, M., Uppgang, S., and Vermet, F. On a model of associative memory with huge storage capacity. *Journal of Statistical Physics*, 168(2):288–299, may 2017. doi: 10.1007/s10955-017-1806-y. URL <https://doi.org/10.1007/s10955-017-1806-y>.
- Devlin, J., Chang, M., Lee, K., and Toutanova, K. BERT: pre-training of deep bidirectional transformers for language understanding. In Burstein, J., Doran, C., and Solorio, T. (eds.), *Proceedings of the 2019 Conference of the North American Chapter of the Association for Computational Linguistics: Human Language Technologies, NAACL-HLT 2019, Minneapolis, MN, USA, June 2-7, 2019, Volume 1 (Long and Short Papers)*, pp. 4171–4186. Association for Computational Linguistics, 2019. doi: 10.18653/v1/n19-1423. URL <https://doi.org/10.18653/v1/n19-1423>.
- Dosovitskiy, A., Beyer, L., Kolesnikov, A., Weissenborn, D., Zhai, X., Unterthiner, T., Dehghani, M., Minderer, M., Heigold, G., Gelly, S., Uszkoreit, J., and Houlsby, N. An image is worth 16x16 words: Transformers for image recognition at scale. In *9th International Conference on Learning Representations, ICLR 2021, Virtual Event, Austria, May 3-7, 2021*. OpenReview.net, 2021. URL <https://openreview.net/forum?id=YicbFdNTTy>.
- Fallah, A., Mokhtari, A., and Ozdaglar, A. E. Generalization of model-agnostic meta-learning algorithms: Recurring and unseen tasks. In Ranzato, M., Beygelzimer, A., Dauphin, Y. N., Liang, P., and Vaughan, J. W. (eds.), *Advances in Neural Information Processing Systems 34: Annual Conference on Neural Information Processing Systems 2021, NeurIPS 2021, December 6-14, 2021, virtual*, pp. 5469–5480, 2021.
- Gärtner, E., Metz, L., Andriluka, M., Freeman, C. D., and Sminchisescu, C. Transformer-based learned optimization. *arXiv preprint arXiv:2212.01055*, 2022.
- Hochreiter, S. and Schmidhuber, J. Long short-term memory. *Neural Comput.*, 9(8):1735–1780, 1997. doi: 10.1162/neco.1997.9.8.1735. URL <https://doi.org/10.1162/neco.1997.9.8.1735>.
- Hochreiter, S., Younger, A. S., and Conwell, P. R. Learning to learn using gradient descent. In Dorffner, G., Bischof, H., and Hornik, K. (eds.), *Artificial Neural Networks - ICANN 2001, International Conference Vienna, Austria, August 21-25, 2001 Proceedings*, volume 2130 of *Lecture Notes in Computer Science*, pp. 87–94. Springer, 2001. doi: 10.1007/3-540-44668-0\_13. URL [https://doi.org/10.1007/3-540-44668-0\\_13](https://doi.org/10.1007/3-540-44668-0_13).
- Hopfield, J. J. Hopfield network. *Scholarpedia*, 2(5):1977, 2007. doi: 10.4249/scholarpedia.1977. URL <https://doi.org/10.4249/scholarpedia.1977>.

- Ichnowski, J., Avigal, Y., Satish, V., and Goldberg, K. Deep learning can accelerate grasp-optimized motion planning. *Science Robotics*, 5(48):eabd7710, 2020.
- Iscen, A., Bird, T., Caron, M., Fathi, A., and Schmid, C. A memory transformer network for incremental learning. *CoRR*, abs/2210.04485, 2022. doi: 10.48550/arXiv.2210.04485. URL <https://doi.org/10.48550/arXiv.2210.04485>.
- James, S., Wohlhart, P., Kalakrishnan, M., Kalashnikov, D., Irpan, A., Ibarz, J., Levine, S., Hadsell, R., and Bousmalis, K. Sim-to-real via sim-to-sim: Data-efficient robotic grasping via randomized-to-canonical adaptation networks. In *IEEE Conference on Computer Vision and Pattern Recognition, CVPR 2019, Long Beach, CA, USA, June 16-20, 2019*, pp. 12627–12637. Computer Vision Foundation / IEEE, 2019. doi: 10.1109/CVPR.2019.01291.
- Kitaev, N., Kaiser, L., and Levskaya, A. Reformer: The efficient transformer. In *8th International Conference on Learning Representations, ICLR 2020, Addis Ababa, Ethiopia, April 26-30, 2020*. OpenReview.net, 2020. URL <https://openreview.net/forum?id=rkgNKkHtvB>.
- Kroto, D. and Hopfield, J. J. Dense associative memory for pattern recognition. In Lee, D. D., Sugiyama, M., von Luxburg, U., Guyon, I., and Garnett, R. (eds.), *Advances in Neural Information Processing Systems 29: Annual Conference on Neural Information Processing Systems 2016, December 5-10, 2016, Barcelona, Spain*, pp. 1172–1180, 2016.
- Kroto, D. and Hopfield, J. J. Large associative memory problem in neurobiology and machine learning. In *9th International Conference on Learning Representations, ICLR 2021, Virtual Event, Austria, May 3-7, 2021*. OpenReview.net, 2021. URL [https://openreview.net/forum?id=X4y\\_100X-hX](https://openreview.net/forum?id=X4y_100X-hX).
- Li, J., Khodak, M., Caldas, S., and Talwalkar, A. Differentially private meta-learning. In *8th International Conference on Learning Representations, ICLR 2020, Addis Ababa, Ethiopia, April 26-30, 2020*. OpenReview.net, 2020. URL <https://openreview.net/forum?id=rJgqMRVYvr>.
- Li, K. and Malik, J. Learning to optimize. In *5th International Conference on Learning Representations, ICLR 2017, Toulon, France, April 24-26, 2017, Conference Track Proceedings*. OpenReview.net, 2017. URL <https://openreview.net/forum?id=ry4Vrt5g1>.
- Li, W. and Todorov, E. Iterative linear quadratic regulator design for nonlinear biological movement systems. In *ICINCO (1)*, pp. 222–229. Citeseer, 2004.
- Liang, J., Saxena, S., and Kroemer, O. Learning active task-oriented exploration policies for bridging the sim-to-real gap. In Toussaint, M., Bicchi, A., and Hermans, T. (eds.), *Robotics: Science and Systems XVI, Virtual Event / Corvallis, Oregon, USA, July 12-16, 2020*, 2020. doi: 10.15607/RSS.2020.XVI.085. URL <https://doi.org/10.15607/RSS.2020.XVI.085>.
- Likhosherstov, V., Choromanski, K., Davis, J., Song, X., and Weller, A. Sub-linear memory: How to make performers slim. *CoRR*, abs/2012.11346, 2020. URL <https://arxiv.org/abs/2012.11346>.
- Likhosherstov, V., Choromanski, K., Dubey, A., Liu, F., Sarlós, T., and Weller, A. Chefs' random tables: Non-trigonometric random features. *to appear at AAAI 2023*, abs/2205.15317, 2022. doi: 10.48550/arXiv.2205.15317. URL <https://doi.org/10.48550/arXiv.2205.15317>.
- Liu, L., Liu, X., Gao, J., Chen, W., and Han, J. Understanding the difficulty of training transformers. In Webber, B., Cohn, T., He, Y., and Liu, Y. (eds.), *Proceedings of the 2020 Conference on Empirical Methods in Natural Language Processing, EMNLP 2020, Online, November 16-20, 2020*, pp. 5747–5763. Association for Computational Linguistics, 2020. doi: 10.18653/v1/2020.emnlp-main.463. URL <https://doi.org/10.18653/v1/2020.emnlp-main.463>.
- Luo, S., Li, S., Cai, T., He, D., Peng, D., Zheng, S., Ke, G., Wang, L., and Liu, T. Stable, fast and accurate: Kernelized attention with relative positional encoding. *CoRR*, abs/2106.12566, 2021. URL <https://arxiv.org/abs/2106.12566>.
- Lv, K., Jiang, S., and Li, J. Learning gradient descent: Better generalization and longer horizons. In Precup, D. and Teh, Y. W. (eds.), *Proceedings of the 34th International Conference on Machine Learning, ICML 2017, Sydney, NSW, Australia, 6-11 August 2017*, volume 70 of *Proceedings of Machine Learning Research*, pp. 2247–2255. PMLR, 2017. URL <http://proceedings.mlr.press/v70/lv17a.html>.
- Metz, L., Maheswaranathan, N., Nixon, J., Freeman, C. D., and Sohl-Dickstein, J. Understanding and correcting pathologies in the training of learned optimizers. In Chaudhuri, K. and Salakhutdinov, R. (eds.), *Proceedings of the 36th International Conference on Machine Learning, ICML 2019, 9-15 June 2019, Long Beach, California, USA*, volume 97 of *Proceedings of Machine Learning Research*, pp. 4556–4565. PMLR, 2019a. URL <http://proceedings.mlr.press/v97/metz19a.html>.

- Metz, L., Maheswaranathan, N., Shlens, J., Sohl-Dickstein, J., and Cubuk, E. D. Using learned optimizers to make models robust to input noise. *CoRR*, abs/1906.03367, 2019b. URL <http://arxiv.org/abs/1906.03367>.
- Metz, L., Maheswaranathan, N., Freeman, C. D., Poole, B., and Sohl-Dickstein, J. Tasks, stability, architecture, and compute: Training more effective learned optimizers, and using them to train themselves. *CoRR*, abs/2009.11243, 2020. URL <https://arxiv.org/abs/2009.11243>.
- Naik, D. K. and Mammone, R. J. Meta-neural networks that learn by learning. [*Proceedings 1992] IJCNN International Joint Conference on Neural Networks*, 1:437–442 vol.1, 1992.
- Pong, V. H., Nair, A. V., Smith, L. M., Huang, C., and Levine, S. Offline meta-reinforcement learning with online self-supervision. In Chaudhuri, K., Jegelka, S., Song, L., Szepesvári, C., Niu, G., and Sabato, S. (eds.), *International Conference on Machine Learning, ICML 2022, 17-23 July 2022, Baltimore, Maryland, USA*, volume 162 of *Proceedings of Machine Learning Research*, pp. 17811–17829. PMLR, 2022. URL <https://proceedings.mlr.press/v162/pong22a.html>.
- Radford, A., Wu, J., Child, R., Luan, D., Amodei, D., and Sutskever, I. Language models are unsupervised multitask learners. 2019.
- Ramsauer, H., Schäfl, B., Lehner, J., Seidl, P., Widrich, M., Gruber, L., Holzleitner, M., Pavlovic, M., Sandve, G. K., Greiff, V., Kreil, D. P., Kopp, M., Klambauer, G., Brandstetter, J., and Hochreiter, S. Hopfield networks is all you need. *CoRR*, abs/2008.02217, 2020. URL <https://arxiv.org/abs/2008.02217>.
- Ravi, S. and Larochelle, H. Optimization as a model for few-shot learning. In *5th International Conference on Learning Representations, ICLR 2017, Toulon, France, April 24-26, 2017, Conference Track Proceedings*. OpenReview.net, 2017. URL <https://openreview.net/forum?id=rJY0-Kcll>.
- Roy, A. and Todorovic, S. Learning to learn second-order back-propagation for cnns using lstms. In *24th International Conference on Pattern Recognition, ICPR 2018, Beijing, China, August 20-24, 2018*, pp. 97–102. IEEE Computer Society, 2018. doi: 10.1109/ICPR.2018.8546078. URL <https://doi.org/10.1109/ICPR.2018.8546078>.
- Roy, A., Saffar, M., Vaswani, A., and Grangier, D. Efficient content-based sparse attention with routing transformers. *Trans. Assoc. Comput. Linguistics*, 9:53–68, 2021. URL <https://transacl.org/ojs/index.php/tacl/article/view/2405>.
- Santoro, A., Bartunov, S., Botvinick, M. M., Wierstra, D., and Lillicrap, T. P. Meta-learning with memory-augmented neural networks. In Balcan, M. and Weinberger, K. Q. (eds.), *Proceedings of the 33nd International Conference on Machine Learning, ICML 2016, New York City, NY, USA, June 19-24, 2016*, volume 48 of *JMLR Workshop and Conference Proceedings*, pp. 1842–1850. JMLR.org, 2016. URL <http://proceedings.mlr.press/v48/santoro16.html>.
- Schlag, I., Irie, K., and Schmidhuber, J. Linear transformers are secretly fast weight programmers. In Meila, M. and Zhang, T. (eds.), *Proceedings of the 38th International Conference on Machine Learning, ICML 2021, 18-24 July 2021, Virtual Event*, volume 139 of *Proceedings of Machine Learning Research*, pp. 9355–9366. PMLR, 2021. URL <http://proceedings.mlr.press/v139/schlag21a.html>.
- Singh, S., Slotine, J.-J., and Sindhwani, V. Optimizing trajectories with closed-loop dynamic sqp. *arXiv preprint arXiv:2109.07081*, 2021.
- Sutton, R. S. Adapting bias by gradient descent: An incremental version of delta-bar-delta. In Swartout, W. R. (ed.), *Proceedings of the 10th National Conference on Artificial Intelligence, San Jose, CA, USA, July 12-16, 1992*, pp. 171–176. AAAI Press / The MIT Press, 1992. URL <http://www.aaai.org/Library/AAAI/1992/aaai92-027.php>.
- Tay, Y., Dehghani, M., Bahri, D., and Metzler, D. Efficient transformers: A survey. *CoRR*, abs/2009.06732, 2020. URL <https://arxiv.org/abs/2009.06732>.
- Tay, Y., Dehghani, M., Abnar, S., Shen, Y., Bahri, D., Pham, P., Rao, J., Yang, L., Ruder, S., and Metzler, D. Long range arena: A benchmark for efficient transformers. In *9th International Conference on Learning Representations, ICLR 2021, Virtual Event, Austria, May 3-7, 2021*. OpenReview.net, 2021. URL <https://openreview.net/forum?id=qVyeW-grC2k>.
- Thrun, S. and Pratt, L. Y. (eds.). *Learning to Learn*. Springer, 1998. ISBN 978-1-4613-7527-2. doi: 10.1007/978-1-4615-5529-2. URL <https://doi.org/10.1007/978-1-4615-5529-2>.
- Vaswani, A., Shazeer, N., Parmar, N., Uszkoreit, J., Jones, L., Gomez, A. N., Kaiser, L., and Polosukhin, I. Attention is all you need. In Guyon, I., von Luxburg, U., Bengio, S., Wallach, H. M., Fergus, R., Vishwanathan, S. V. N., and Garnett, R. (eds.), *Advances in Neural Information Processing Systems 30: Annual Conference on Neural*

- Information Processing Systems 2017, December 4-9, 2017, Long Beach, CA, USA*, pp. 5998–6008, 2017.
- Vicol, P., Metz, L., and Sohl-Dickstein, J. Unbiased gradient estimation in unrolled computation graphs with persistent evolution strategies. In Meila, M. and Zhang, T. (eds.), *Proceedings of the 38th International Conference on Machine Learning, ICML 2021, 18-24 July 2021, Virtual Event*, volume 139 of *Proceedings of Machine Learning Research*, pp. 10553–10563. PMLR, 2021. URL <http://proceedings.mlr.press/v139/vicol21a.html>.
- Wang, S., Li, B. Z., Khabsa, M., Fang, H., and Ma, H. Linformer: Self-attention with linear complexity. *CoRR*, abs/2006.04768, 2020. URL <https://arxiv.org/abs/2006.04768>.
- Wichrowska, O., Maheswaranathan, N., Hoffman, M. W., Colmenarejo, S. G., Denil, M., de Freitas, N., and Sohl-Dickstein, J. Learned optimizers that scale and generalize. In Precup, D. and Teh, Y. W. (eds.), *Proceedings of the 34th International Conference on Machine Learning, ICML 2017, Sydney, NSW, Australia, 6-11 August 2017*, volume 70 of *Proceedings of Machine Learning Research*, pp. 3751–3760. PMLR, 2017. URL <http://proceedings.mlr.press/v70/wichrowska17a.html>.
- Xiao, X., Zhang, T., Choromanski, K., Lee, T. E., Francis, A. G., Varley, J., Tu, S., Singh, S., Xu, P., Xia, F., Persson, S. M., Kalashnikov, D., Takayama, L., Frostig, R., Tan, J., Parada, C., and Sindhwan, V. Learning model predictive controllers with real-time attention for real-world navigation. *CoRR*, abs/2209.10780, 2022. doi: 10.48550/arXiv.2209.10780. URL <https://doi.org/10.48550/arXiv.2209.10780>.
- Yao, H., Zhang, L., and Finn, C. Meta-learning with fewer tasks through task interpolation. In *The Tenth International Conference on Learning Representations, ICLR 2022, Virtual Event, April 25-29, 2022*. OpenReview.net, 2022. URL <https://openreview.net/forum?id=ajXWF7bVR8d>.
- Younger, A. S., Hochreiter, S., and Conwell, P. R. Meta-learning with backpropagation. *IJCNN'01. International Joint Conference on Neural Networks. Proceedings (Cat. No.01CH37222)*, 3:2001–2006 vol.3, 2001.
- Zaheer, M., Guruganesh, G., Dubey, K. A., Ainslie, J., Alberti, C., Ontanon, S., Pham, P., Ravula, A., Wang, Q., Yang, L., et al. Big bird: Transformers for longer sequences. *Advances in Neural Information Processing Systems*, 33:17283–17297, 2020.
- Zhao, Z., Nagabandi, A., Rakelly, K., Finn, C., and Levine, S. MELD: meta-reinforcement learning from images via latent state models. In Kober, J., Ramos, F., and Tomlin, C. J. (eds.), *4th Conference on Robot Learning, CoRL 2020, 16-18 November 2020, Virtual Event / Cambridge, MA, USA*, volume 155 of *Proceedings of Machine Learning Research*, pp. 1246–1261. PMLR, 2020. URL <https://proceedings.mlr.press/v155/zhao21d.html>.

## A. Appendix

### A.1. The proof of Theorem 4.4

*Proof.* Take a memory  $\xi^l \in \{-1, +1\}^N$  and an input  $\widehat{\xi}^l \in \mathcal{B}(\xi^l, \rho N)$ . Denote by  $\text{neg}(\widehat{\xi}^l, i)$  a vector obtained from  $\widehat{\xi}^l$  by replacing  $\widehat{\xi}^l(i)$  with  $-\widehat{\xi}^l(i)$ . Let us study the change of the energy of the system as we flip the value of the  $i$ th dimension of the input  $\widehat{\xi}^l$  since the sign of this change solely determines the update that will be made. We have the following:

$$\Delta(E_{\text{rand}}) = E(\text{neg}(\widehat{\xi}^l, i); \xi^1, \dots, \xi^M) - E(\widehat{\xi}^l; \xi^1, \dots, \xi^M) = E_{\text{signal}} + E_{\text{noise}}, \quad (19)$$

where:

$$E_{\text{signal}} = \frac{1}{r} \sum_{k=1}^r (W_k^l - Z_k^l), \quad (20)$$

$$E_{\text{noise}} = \frac{1}{r} \sum_{k=1}^r \sum_{\mu \in \{1, \dots, M\} \setminus \{l\}} (W_k^\mu - Z_k^\mu), \quad (21)$$

and furthermore:  $W_k^i = a_k^i b_k$ ,  $Z_k^i = a_k^i c_k$  for:

$$\begin{aligned} a_k^i &= D \exp\left(-\frac{N}{2}\right) \exp(B\omega_k^\top \xi^i - \widehat{A}\|\omega_k\|_2^2), \\ b_k &= D \exp\left(-\frac{N}{2}\right) \exp(B\omega_k^\top \widehat{\xi}^l - \widehat{A}\|\omega_k\|_2^2), \\ c_k &= D \exp\left(-\frac{N}{2}\right) \exp(B\omega_k^\top \text{neg}(\widehat{\xi}^l, i) - \widehat{A}\|\omega_k\|_2^2). \end{aligned} \quad (22)$$

If  $\omega_1, \dots, \omega_r \sim \mathcal{N}(0, \mathbf{I}_N)$  then, from the fact that  $E_{\text{rand}}$  is the unbiased estimation of  $E_{\text{reg}}$ , we get:

$$\begin{aligned} \mathbb{E}[X_k] &= \exp((\xi^l)^\top \widehat{\xi}^l), \\ \mathbb{E}[Y_k] &= \exp((\xi^l)^\top \text{neg}(\widehat{\xi}^l, i)), \\ \mathbb{E}[W_k^\mu] &= \exp((\xi^\mu)^\top \widehat{\xi}^l), \\ \mathbb{E}[Z_k^\mu] &= \exp((\xi^\mu)^\top \text{neg}(\widehat{\xi}^l, i)), \end{aligned} \quad (23)$$

This is a direct consequence of the OPRF-mechanism introduced in (Likhosherstov et al., 2022). Variables:  $X_k$ ,  $Y_k$ ,  $W_k^\mu$  and  $Z_k^\mu$  for  $\mu = 1, \dots, M$  are simply unbiased estimators of the softmax-kernel values obtained via applying OPRF-mechanism. Let us now compute the expected change of the energy of the system:

$$\mathbb{E}[\Delta(E_{\text{rand}})] = \mathbb{E}[E_{\text{signal}}] + \mathbb{E}[E_{\text{noise}}], \quad (24)$$

where:

$$\mathbb{E}[E_{\text{signal}}] = \frac{1}{r} \sum_{k=1}^r (\mathbb{E}[X_k] - \mathbb{E}[Y_k]) = \frac{1}{r} \sum_{k=1}^r \left( \exp((\xi^l)^\top \widehat{\xi}^l) - \exp((\xi^l)^\top \text{neg}(\widehat{\xi}^l, i)) \right) \quad (25)$$

and

$$\begin{aligned} \mathbb{E}[E_{\text{noise}}] &= \frac{1}{r} \sum_{k=1}^r \sum_{\mu \in \{1, \dots, M\} \setminus \{l\}} (\mathbb{E}[W_k^\mu] - \mathbb{E}[Z_k^\mu]) = \\ &= \frac{1}{r} \sum_{k=1}^r \sum_{\mu \in \{1, \dots, M\} \setminus \{l\}} \left( \exp((\xi^\mu)^\top \widehat{\xi}^l) - \exp((\xi^\mu)^\top \text{neg}(\widehat{\xi}^l, i)) \right) \end{aligned} \quad (26)$$

We will first upper bound  $|\mathbb{E}[E_{\text{noise}}]|$ . We have:

$$\begin{aligned}
|\mathbb{E}[E_{\text{noise}}]| &\leq \frac{1}{r} \sum_{k=1}^r \sum_{\mu \in \{1, \dots, M\} \setminus \{l\}} \left( \exp((\xi^\mu)^\top \hat{\xi}^l) + \exp((\xi^\mu)^\top \text{neg}(\hat{\xi}^l, i)) \right) \\
&\leq \sum_{k=1}^r \sum_{\mu \in \{1, \dots, M\} \setminus \{l\}} \left( \exp(N(1 - 2(\tau - \rho))) + \exp(N(1 - 2(\tau - \rho) + \frac{2}{N})) \right) \\
&\leq 2M \exp(N(1 - 2(\tau - \rho) + \frac{2}{N}))
\end{aligned} \tag{27}$$

We will now consider two cases:

**Case 1:**  $\hat{\xi}^l(i) = \xi^l(i)$ :

In this setting, flipping the value of the  $i$ th dimension of the input vector increases its distance from the close neighbor. Therefore in this case we would like the energy change of the system to be positive (so that the flip does not occur). From the Equation 25, we obtain:

$$\begin{aligned}
\mathbb{E}[E_{\text{signal}}] &\geq \frac{1}{r} \sum_{k=1}^r (\exp(N(1 - 2\rho)) - \exp(N(1 - 2\rho) - 2)) = \\
&\quad \exp(N(1 - 2\rho))(1 - e^{-2})
\end{aligned} \tag{28}$$

Thus we obtain:

$$\mathbb{E}[\Delta(E_{\text{rand}})] \geq \exp(N(1 - 2\rho))(1 - e^{-2}) - 2M \exp(N(1 - 2(\tau - \rho) + \frac{2}{N})) \tag{29}$$

Therefore, if the following holds:

$$M \leq \exp(2N(\tau - 2\rho)) \frac{1 - e^{-2}}{2e^2}, \tag{30}$$

then  $\mathbb{E}[\Delta(E_{\text{rand}})] > 0$ .

**Case 2:**  $\hat{\xi}^l(i) = -\xi^l(i)$ :

In this setting, flipping the value of the  $i$ th dimension of the input vector decreases its distance from the close neighbor. Therefore in this case we would like the energy change of the system to be negative (so that the flip does not occur). From the Equation 25, we obtain:

$$\begin{aligned}
\mathbb{E}[E_{\text{signal}}] &\leq \frac{1}{r} \sum_{k=1}^r (\exp(N(1 - 2\rho)) - \exp(N(1 - 2\rho) + 2)) = \\
&\quad \exp(N(1 - 2\rho))(1 - e^2)
\end{aligned} \tag{31}$$

Thus we obtain:

$$\mathbb{E}[\Delta(E_{\text{rand}})] \leq \exp(N(1 - 2\rho))(1 - e^2) + 2M \exp(N(1 - 2(\tau - \rho) + \frac{2}{N})) \tag{32}$$

Therefore, if the following holds:

$$M \leq \exp(2N(\tau - 2\rho)) \frac{e^2 - 1}{2e^2}, \tag{33}$$

then  $\mathbb{E}[\Delta(E_{\text{rand}})] < 0$ . Note that the bound from Inequality 30 is stronger than the one from Inequality 33. That completes the proof of the first part of the theorem.

Now we will compute the variance of  $\Delta(E_{\text{rand}})$ . Denote:

$$Z_k = \sum_{\mu \in \{1, \dots, M\}} (W_k^\mu - Z_k^\mu) \quad (34)$$

Note that if  $\omega_1, \dots, \omega_r$  are chosen independently then  $Z_k$  for  $k = 1, \dots, r$  are independent. The following is true:

$$\begin{aligned} \text{Var}(\Delta(E_{\text{rand}})) &= \text{Var}(E_{\text{signal}} + E_{\text{noise}}) = \text{Var}\left(\frac{1}{r} \sum_{k=1}^r \sum_{\mu \in \{1, \dots, M\}} (W_k^\mu - Z_k^\mu)\right) \\ &= \text{Var}\left(\frac{1}{r} \sum_{k=1}^r Z_k\right) = \frac{1}{r^2} \sum_{k=1}^r \text{Var}(Z_k) = \frac{1}{r^2} \sum_{k=1}^r \text{Var}\left(\sum_{\mu \in \{1, \dots, M\}} (W_k^\mu - Z_k^\mu)\right) \\ &= \frac{1}{r^2} \sum_{k=1}^r \left( \mathbb{E}\left[\left(\sum_{\mu \in \{1, \dots, M\}} (W_k^\mu - Z_k^\mu)\right)^2\right] - \left(\mathbb{E}\left[\sum_{\mu \in \{1, \dots, M\}} (W_k^\mu - Z_k^\mu)\right]\right)^2 \right) \end{aligned} \quad (35)$$

Therefore we have:

$$\begin{aligned} \text{Var}(\Delta(E_{\text{rand}})) &= \frac{1}{r^2} \sum_{k=1}^r \left( \sum_{\mu_1, \mu_2 \in \{1, \dots, M\}} \mathbb{E}[W_k^{\mu_1} W_k^{\mu_2}] + \sum_{\mu_1, \mu_2 \in \{1, \dots, M\}} \mathbb{E}[Z_k^{\mu_1} Z_k^{\mu_2}] \right. \\ &\quad \left. - \frac{2}{r^2} \sum_{k=1}^r \sum_{\mu_1, \mu_2 \in \{1, \dots, M\}} \mathbb{E}[W_k^{\mu_1} Z_k^{\mu_2}] \right. \\ &\quad \left. - \frac{1}{r^2} \sum_{k=1}^r \left( \sum_{\mu_1, \mu_2 \in \{1, \dots, M\}} \mathbb{E}[W_k^{\mu_1}] \mathbb{E}[W_k^{\mu_2}] + \sum_{\mu_1, \mu_2 \in \{1, \dots, M\}} \mathbb{E}[Z_k^{\mu_1}] \mathbb{E}[Z_k^{\mu_2}] \right) \right. \\ &\quad \left. - \frac{2}{r^2} \sum_{k=1}^r \sum_{\mu_1, \mu_2 \in \{1, \dots, M\}} \mathbb{E}[W_k^{\mu_1}] \mathbb{E}[Z_k^{\mu_2}] \right) \end{aligned} \quad (36)$$

Note that from the fact that our random feature map based estimators are unbiased, we get (as we already noted before in Equation 23 and put here again for Reader's convenience):

$$\begin{aligned} \mathbb{E}[W_k^\mu] &= \exp((\xi^\mu)^\top \hat{\xi}^l), \\ \mathbb{E}[Z_k^\mu] &= \exp((\xi^\mu)^\top \text{neg}(\hat{\xi}^l, i)), \end{aligned} \quad (37)$$

Let us now define:

$$\Psi(\mathbf{x}) = D^4 \exp(-2N) \exp(B\omega^\top \mathbf{x} - 4\hat{A}\|\omega\|_2^2). \quad (38)$$

Note that the following is true:

$$\begin{aligned} \mathbb{E}[W_k^{\mu_1} W_k^{\mu_2}] &= \Psi(\xi^{\mu_1} + \xi^{\mu_2} + 2\hat{\xi}^l) \\ \mathbb{E}[Z_k^{\mu_1} Z_k^{\mu_2}] &= \Psi(\xi^{\mu_1} + \xi^{\mu_2} + 2\text{neg}(\hat{\xi}^l, i)) \\ \mathbb{E}[W_k^{\mu_1} Z_k^{\mu_2}] &= \Psi(\xi^{\mu_1} + \xi^{\mu_2} + \hat{\xi}^l + \text{neg}(\hat{\xi}^l, i)) \end{aligned} \quad (39)$$

Thus it remains to find closed-form formula for  $\Psi(\mathbf{x})$  for any given  $\mathbf{x} \in \mathbb{R}^N$ .

From the proof of Theorem 3.1 in (Likhosherstov et al., 2022), we get for  $A < 0$ :

$$\mathbb{E}[\exp(A\|\omega\|^2 + B\omega^\top \mathbf{x})] = (1 - 2A)^{-\frac{N}{2}} \exp\left(\frac{B^2}{2(1 - 2A)} \|\mathbf{x}\|^2\right) \quad (40)$$

Thus we obtain:

$$\Psi(\mathbf{x}) = D^4 \exp(-2N) (1 + 8\hat{A})^{-\frac{N}{2}} \exp\left(\frac{B^2}{2(1 - 8\hat{A})} \|\mathbf{x}\|^2\right) \quad (41)$$

Plugging to Equation 36 formulae from Equation 37 and Equation 39 and utilizing Equation 41 for  $\Psi$ , we obtain the formula for the variance from the statement of the Theorem.  $\square$

## A.2. Compute Resources Used

All Mnemosyne optimizer variants were trained and tested on a TPU pod containing 4 TPU v3 chips with JAX. Hundreds of rounds of training and inference were needed to compare different variations, tasks and meta-losses. Transformers architectures have revolutionized the field of machine learning yet they should be applied cautiously given the carbon emission footprint of their training.